Geophysical Journal International

Geophys. J. Int. (2011) doi: 10.1111/j.1365-246X.2011.05011.x

On the visibility of the inner-core shear wave phase *PKJKP* at long periods

Peter M. Shearer,[1] Catherine A. Rychert[2] and Qinya Liu[3]

[1] *Institute of Geophysics and Planetary Physics, Scripps Institution of Oceanography, University of California, San Diego,* 9500 *Gilman Drive M/C* 0225, *La Jolla, CA* 92093, *USA. E-mail: pshearer@ucsd.edu*

[2] *Department of Earth Science, University of Bristol, Wills Memorial Building, Queen's Road, Bristol* BS8 1RJ, *UK*

[3] *Department of Physics, University of Toronto,* 60 *St. George St., Toronto, M5S* 1A7 *Ontario, Canada*

Accepted 2011 March 7. Received 2011 March 4; in original form 2010 November 18

SUMMARY

Stacks of over 90 000 long-period seismograms recorded by the global seismic networks resolve many seismic phases but fail to detect the inner-core shear phase *PKJKP*. We compare these results to synthetic seismograms computed for PREM using the spectral-element method and show that expected *PKJKP* amplitudes are over 10 times smaller than signal-generated 'noise' caused by high-order *P* surface multiples and reverberations from upper-mantle discontinuities. Indeed, *PKJKP* can only be seen in synthetic seismograms when differences are taken between two sets of synthetics generated from Earth models with slightly different inner-core shear velocities. These results suggest that routine observation of *PKJKP* is unlikely and that reported observations, if real, must have resulted from exceptional focusing effects or inner-core attenuation much less that current models.

Key words: Core, outer core and inner core; Body waves; Computational seismology; Wave propagation.

INTRODUCTION

The solidity of the inner core is well-established from normal-mode studies (e.g. Dziewonski & Gilbert 1971; Masters & Shearer 1990; Deuss 2008) and the observed amplitude of the inner-core boundary (ICB) reflected phase *PKiKP* (e.g. Cummins & Johnson 1988; Shearer & Masters 1990; Koper & Pyle 2004). However, these results do not provide precise values for the inner-core *S* velocity, nor do they constrain very well its depth dependence within the inner core or the size of any possible shear wave splitting caused by inner-core anisotropy. The body-wave phase *PKJKP*, which contains an *S*-wave leg through the inner core, could potentially provide more information. However, observations of this phase have proven difficult and often controversial. Doornbos (1974) showed that its predicted amplitude is very small, owing to small *P*-to-*S* and *S*-to-*P* transmission coefficients at the ICB and strong inner-core attenuation, and that observations are likely impossible, at least at short periods, given realistic levels of Earth noise.

A few recent studies have revisited this issue by presenting evidence for *PKJKP* and related phases. Okal & Cansi (1998) applied a stacking method to records at 2–10 s period from 8 stations recording the 1996 Flores Sea earthquake (584 km deep, M_w 7.9) and imaged an apparent arrival consistent with an inner-core *S* velocity of 3.65 km s^{-1}. Deuss *et al.* (2000) applied a different stacking method to records filtered to 10–100 s from 47 stations for the same Flores Sea event and detected apparent *pPKJKP* and *SKJKP* arrivals consistent with an inner-core *S* velocity of 3.6 km s^{-1}. Cao *et al.* (2005) stacked records (filtered from 10 to 17 s period) of the Gräfenberg Seismic Array in Germany from a 1999 earthquake in Melanesia (76 km deep, M_w 7.3) and found an apparent *PKJKP* arrival close to the time predicted by the PREM model (Dziewonski & Anderson 1981), which has an average inner-core *S* velocity of about 3.6 km s^{-1}.

Both Deuss *et al*. and Cao *et al*. computed long-period synthetic seismograms to test their observations and noted the difficulty in observing *PKJKP* even in synthetics because its predicted amplitude is much lower than other arrivals in the same time window. These weak *PKJKP* amplitudes become even more pronounced at shorter periods and both studies argued that detection of *PKJKP* at periods below about 10 s is unlikely. However, Wookey & Helffrich (2008) stacked 704 short-period records from the Japanese Hi-Net array from a 2006 earthquake in Mozambique (11 km deep, *M* 7.0) and detected an apparent *PKJKP* arrival with timing and slowness consistent with predictions of standard Earth models. However, its amplitude was much larger than synthetic predictions, unless large changes are made to inner-core attenuation, anisotropy or *P*-velocity structure.

Our purpose here is not to revisit these earlier studies in detail, but to explore whether *PKJKP* might be observed more routinely. Observations to date appear to require special circumstances—the rare earthquake or ray path geometry that produces anomalously large *PKJKP* arrivals, that is, paths in which *PKJKP* is visible, as contrasted with the vast majority of paths where it is not. This is not very satisfactory from the point of view of constraining

inner-core properties because anomalous observations do not necessarily provide unbiased information. For example (optimistically), they could represent special ray paths in which focusing effects have created a detection 'sweet spot' with large *PKJKP* amplitudes. Or (pessimistically), they could represent random scattered arrivals from deep Earth heterogeneity that occasionally land in the right place to be misinterpreted as *PKJKP*. Because the observations are so rare, issues of selection bias are hard to avoid. There are few published accounts of failures to detect *PKJKP* (one exception is Kawakatsu 1992). Thus, it would be preferable if *PKJKP* could be observed by stacking all the available seismic data, rather than a small fraction of the data. The purpose of this paper is to test whether this is a realistic goal.

STACKING GLOBAL SEISMIC DATA

PKJKP has an unusual ray path geometry (see Fig. 1) that results from the low shear velocity in the inner core. Predicted *PKJKP* arrivals are at about 28 to 30 min and span distances from 180° to over 270° from the source (distance taken in the direction of the *P* wave leaving the source). Owing to the internal caustic surface in the inner core, *PKJKP* is Hilbert transformed compared to direct *P* arrivals. Because *P*-to-*S* and *S*-to-*P* transmission coefficients go to zero at normal incidence, *PKJKP* should vanish at 180°. For an inner-core shear velocity of 3.6 km s^{-1} (i.e. close to PREM), *PKJKP* amplitudes are expected to be largest at about 120–150° (Doornbos 1974). Reported *PKJKP* observations have been at 113–119° (Okal & Cansi 1998), 110–175° (Deuss *et al.* 2000), ∼140° (Cao *et al.* 2005) and 106–120° (Wookey & Helffrich 2008). At these distances, *PKJKP* arrives late in the wedge of body-wave phases that arrive before the surface waves. Long-period data stacks generally show far more seismic phases in this part of the wavefield than equivalent short-period stacks (e.g. Astiz *et al.* 1996). This is mainly because of the effect of attenuation on high-frequency *S* waves and *P* surface multiples (which travel through the more-attenuating upper mantle multiple times). Similarly, given estimated values of inner-core attenuation, *PKJKP* amplitudes are expected to be much larger at long periods.

Here, we apply a reference phase stacking method that has been used successfully to resolve upper-mantle discontinuity phases in long-period seismograms (e.g. Shearer 1991). To image the wavefield between 100 and 180° near the expected arrival times of *PKJKP*, we find that *PP* (along its minor arc) is a convenient reference phase because it spans this distance interval and is generally well-observed (see Fig. 1 for an example *PP* ray path). We decided against using *PKP* as a reference phase, even though it has takeoff angles closer to *PKJKP* than *PP*, because its multiple branches and large amplitude variations would complicate the analysis. We use the IRIS FARM from 1990 to 2004. We start with 120 500 vertical-component seismograms that have a local *PP* signal-to-noise ratio of two or greater after a bandpass filter (15–100 s) is applied. Of these, we use 90 673 seismograms from 3648 shallow earthquakes (<50 km). We time shift and stack the original broadband seismograms based on the time of the maximum *PP* amplitude (as measured at 10–100 s period), flipping the polarity if necessary. Although the source-time functions of the different events in each distance bin will vary, this stacking method nonetheless yields very similar effective source-time functions when large numbers of events are processed (Shearer 1991). The reference phase stacking method provides only an approximate waveform alignment for other seismic phases. However, at long-periods (>15 s) the method works well in practice because the timing differences among different phases due to ellipticity and 3-D structure are generally less than the dominant period of the data.

Fig. 2 shows the resulting image, with positive amplitudes plotted in blue and negative amplitudes plotted in red. Many standard seismic phases are visible, as well as mantle discontinuity phases (i.e. from the 410–660 km velocity jumps), which appear as 'railroad track' features before and after the *P* surface multiples. The two curved lines show predicted arrival times for *PKJKP* for models in which the inner-core *S* velocity is 10 per cent faster and 10 per

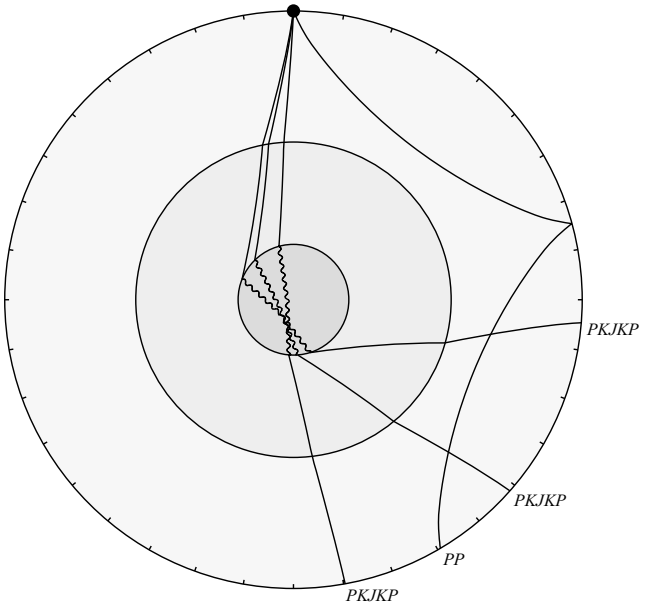

Figure 1. *PKJKP* and *PP* ray paths. Solid lines show *P*-wave legs through the outer core and mantle; wiggly lines show the *S*-wave legs through the inner core. Tic marks are every 10° in source–receiver distance.

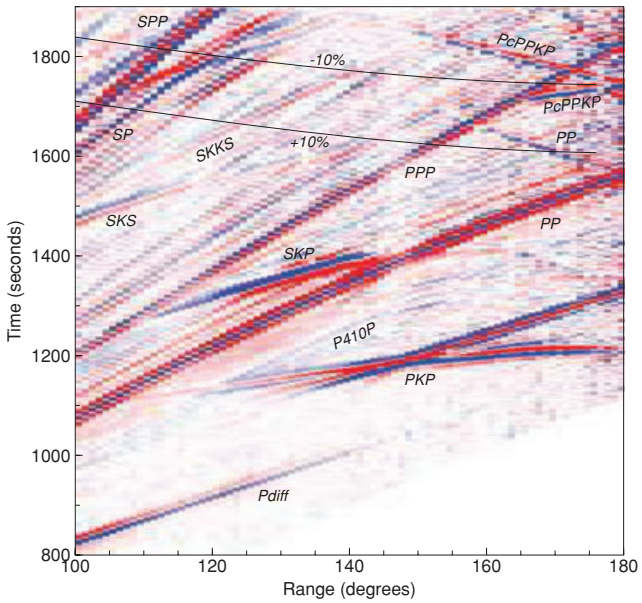

Figure 2. A stack of 90 673 seismograms from 3648 shallow earthquakes (<50 km). Amplitudes and times are relative to the *PP* phase. Positive amplitudes are plotted in blue, negative amplitudes in red. Major phase names are labelled. The curves show predicted *PKJKP* traveltime curves for inner-core *S* velocities ±10 per cent compared to the PREM values.

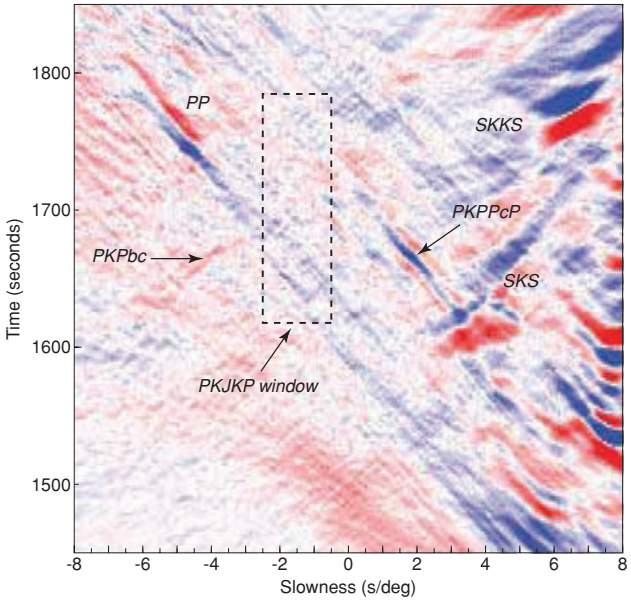

Figure 3. A slant stack image of the data stack of Fig. 2. Times are relative to a reference distance of 140°. The major phase arrivals are labelled. The box shows the expected window for *PKJKP* arrivals for inner-core *S* velocities within 10 per cent of the PREM values.

cent slower than PREM. Thus, the PREM-predicted *PKJKP* phase should lie midway between and parallel to these lines, which have slightly negative slope. However, no matching phase is visible in this region, in which the wavefield is dominated by the positive-slope arrivals of the high-order *P* surface multiples and mantle reverberations.

Often the visibility of weak arrivals can be enhanced by applying slant-stacking methods. Fig. 3 shows the application of slant stacking to the waveform stack of Fig. 2. To avoid truncation artefacts, half-cos^2 tapers are applied between 100 and 110° and between 170 and 180°. We experimented with nth root stacking to normalize the amplitude information. Fig. 3 shows results for $n = 5$, but results for other n values are very similar. Most of the resolved phases in the slant stack are also seen in the record-section image; the one exception is a weak *PKPbc* arrival that can be resolved only in the slant-stack image. We were not able to find any set of slant stacking parameters for which *PKJKP* is visible within the window defined by ±10 per cent *S* velocity perturbations from PREM. It is possible that the visibility of *PKJKP* in the data stacks has been reduced by 3-D mantle and inner-core structure (heterogeneity and anisotropy) if its effects are strong enough to cause variations in the traveltimes of *PKJKP* relative to *PP* larger than the dominant period of the data. However, it is not necessary to assume this has occurred to explain the absence of *PKJKP* in the data stacks because it also cannot be seen in synthetics computed from a 1-D Earth model without any lateral heterogeneity or anisotropy (see below).

We note that even with uniformly sampled data (every degree in distance) and our tapering to avoid edge effects, the slant-stack image contains a number of streaking artefacts. These artefacts are likely to be even stronger in single-event stacks recorded by irregularly spaced stations.

SYNTHETIC SEISMOGRAMS

Both Deuss *et al.* (2000) and Cao *et al.* (2005) have noted the difficulty of seeing *PKJKP* in synthetic seismograms (computed at long periods using normal-mode summation) because of its weak amplitude and interference from other phases. To test this, we compute synthetic seismograms for the 1-D PREM model using the spectral-element method (SEM). SEMs combine the geometrical flexibility of finite-element methods with an accurate representation of the wavefield by high-order Lagrange polynomials, and have been successfully applied to simulations of global seismic wave propagation (e.g. Komatitsch & Tromp 2002a,b; Chaljub *et al.* 2003). The accuracy of the methods has been verified with benchmarks against normal-mode synthetics for the PREM model (Komatitsch & Tromp 2002a). Here, we compute 40-min SEM synthetics for periods of 17 s and longer at 1° epicentral intervals from a 20 km deep isotropic source.

To compare with our data stack, we normalize the synthetic amplitudes using the *PP* phase and plot them at the same scale (Fig. 4). The result appears very similar to the observations and most of the phases are well matched in appearance and relative amplitude. However, there are some exceptions. 220-km discontinuity phases are apparent in the synthetics (caused by the 220 km discontinuity in PREM) but absent in the data stacks, suggesting that the 220 km discontinuity is not a globally coherent feature (as noted by Shearer 1990). The core diffracted phases *PPdiff* (*PP* beyond 200°) and *PKPdiff* are more visible in the synthetics than in the data. This may be caused by lateral heterogeneity in the vicinity of the core–mantle boundary (CMB), the effects of which are not included in the 1-D PREM model used to generate the synthetics. CMB structure should not, however, have as strong an effect on *PKJKP* as on the diffracted phases, because its rays cross the CMB at relatively steep angles. A slant stack of the synthetics, processed in the same way as the real data, is shown in Fig. 5. *PKJKP* is not visible in the synthetics in either the record section or the slant-stack image.

We experimented with various approaches to make *PKJKP* visible in the synthetics, including: (1) we turned off inner-core

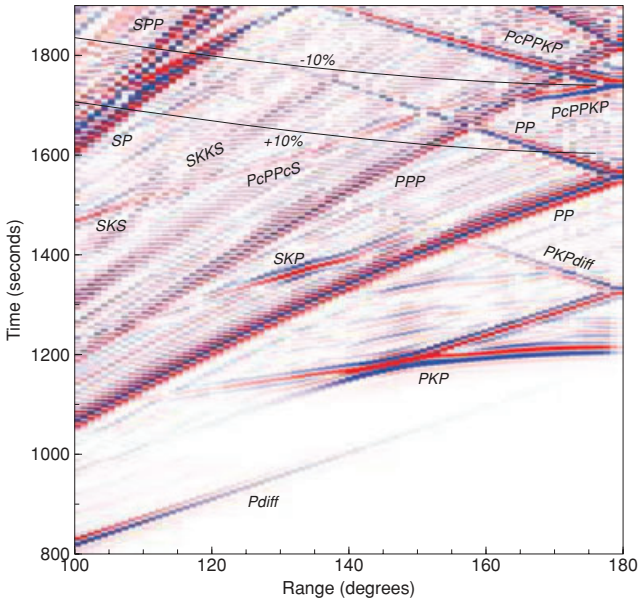

Figure 4. Synthetic seismograms computed from PREM using the spectral element method for an isotropic source at 20 km depth. Amplitudes and times are relative to the *PP* phase. Positive amplitudes are plotted in blue, negative amplitudes in red. Major phase names are labelled. The curves show predicted *PKJKP* traveltime curves for inner-core *S* velocities ±10 per cent compared to the PREM values.

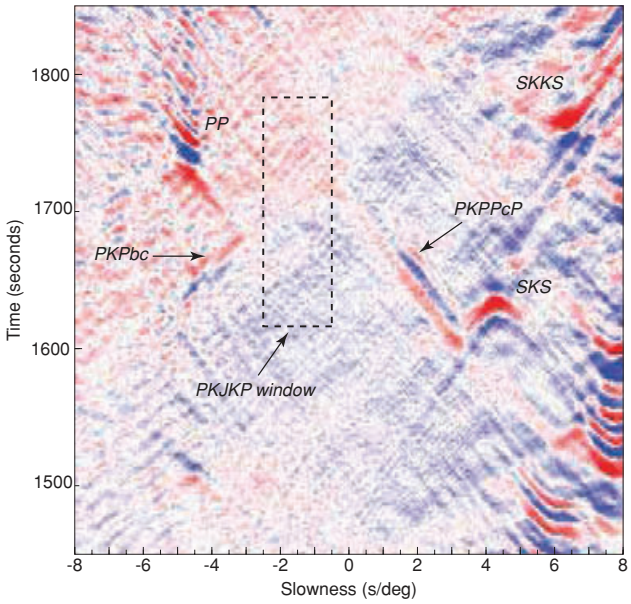

Figure 5. A slant stack image of the data stack of Fig. 4. Times are relative to a reference distance of 140°. The major phase arrivals are labelled. The box shows the expected window for *PKJKP* arrivals for inner-core *S* velocities within 10 per cent of the PREM values.

attenuation. This is physically unrealistic because normal mode observations require relatively low Q_β in the inner core (e.g. Masters & Shearer 1990). However, at these observation periods even infinite *Q* does not increase *PKJKP* amplitudes very much. The main problem is the low values of the transmission coefficients at the ICB. (2) Because the obscuring phases are mainly high-order *P* surface multiples, which leave the source less steeply and in the opposite direction as the *PKJKP* rays, we tried a double-couple dip-slip source oriented so that a node in its *P* radiation pattern corresponded to the takeoff angle for *PPPP* at 130°. This should send proportionally much more energy at *PKJKP* takeoff angles compared to the *P* surface multiples. These synthetics look different from those plotted in Fig. 4 but do not show *PKJKP* arrivals. (3) We also tried a deep source at 600 km depth, which produced numerous depth phases, but no visible *PKJKP* or *pPKJKP* arrivals. (4) Following Deuss *et al.* (2000), we computed synthetics for a liquid inner core and took the difference between the PREM synthetics and the liquid core synthetics. This produced large differences in many phases that interact with the inner core, including *PKKPdf* and *PcPPKP*, which arrive near the predicted time for *PKJKP*. However, *PKJKP* itself was not obvious in the differential waveform image.

The approach that worked best was to compute synthetics for an inner core 10 per cent faster than PREM and then take the difference between these synthetics and the PREM synthetics (a similar test was performed by Cao *et al*. 2005). These results are plotted in Fig. 6, assuming infinite inner-core *Q*. Perturbing the inner-core shear velocity produces observable changes in *PKJKP*, as well as *PKPdf* and *PKIIKP* (in the latter cases, this is caused by changes to the transmission and reflection coefficients at the ICB). But these changes for *PKJKP* are of very small amplitude compared to the interfering phases, as is made clear by Fig. 7, which compares the PREM synthetics to those with 10 per cent faster inner-core *S* velocities, at distances between 135 and 140°. This plot shows how hard observing *PKJKP* will be, assuming it has amplitudes comparable to those predicted by standard 1-D Earth models like PREM. The problem is the low amplitude of *PKJKP* compared to the signal-generated 'noise' of the high-order *P* surface multiples and discontinuity reverberations.

DISCUSSION

This paper describes what might be termed a negative result—we fail to detect *PKJKP* in stacks of global seismic data. A similar result was obtained by Kawakatsu (1992) based on the global seismic data available at that time. However, our results should nonetheless be useful as a guide for future seismologists who may have similar ideas and to put previous observations in perspective. Given that routine detection of *PKJKP* appears very difficult, what can be done to move beyond the reported isolated observations? One approach would be to examine the previous detections more carefully to see if *PKJKP* can be seen along similar ray paths, to see how narrow the observation window might be. Another approach would be to recognize that *PKJKP* detections probably have resulted from searches targeted in the expected *PKJKP* time/slowness window rather than more comprehensive analyses of the entire seismic wavefield. Mantle scattering can sometimes cause anomalous arrivals in unexpected places (e.g. Kawakatsu & Niu 1994). Searching the seismic wavefield systematically for these arrivals would help determine how common they are and whether some of the previous *PKJKP* observations may have resulted from the random occurrence of a scattered phase in the *PKJKP* observation window.

Finally, we should note that our results are for long-period seismograms and are most relevant to the Okal & Cansi (1998), Deuss *et al.* (2000) and Cao *et al.* (2005) papers reporting *PKJKP* observations at similar periods. The recent Wookey & Helffrich (2008) paper is different because it finds evidence for *PKJKP* in short-period data. If these observations are correct, then inner-core Q_β is likely much higher than PREM values, at least for certain paths (see discussion in Wookey and Helffrich). In this case, *PKJKP* might well be easier to observe at short periods than long periods, not because *PKJKP* amplitudes are greater but because the amplitudes of the interfering *P* surface multiples and reverberations are greatly

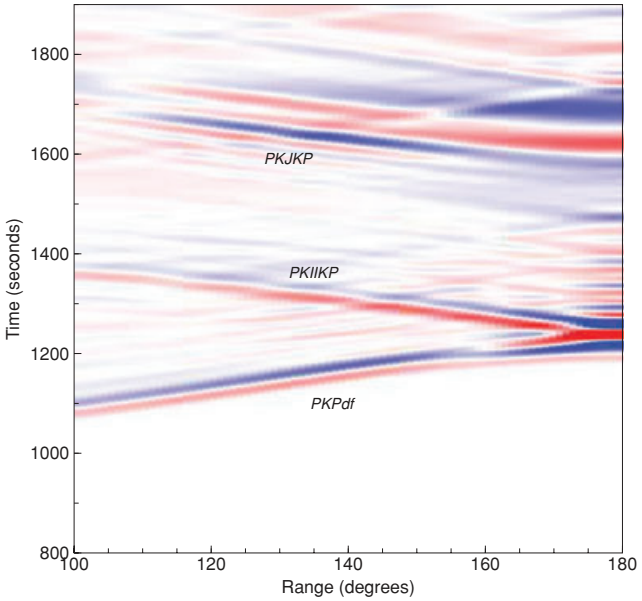

Figure 6. The difference between synthetic seismograms computed for an inner core with *S* velocity 10 per cent greater than PREM and the PREM synthetics of Fig. 4.

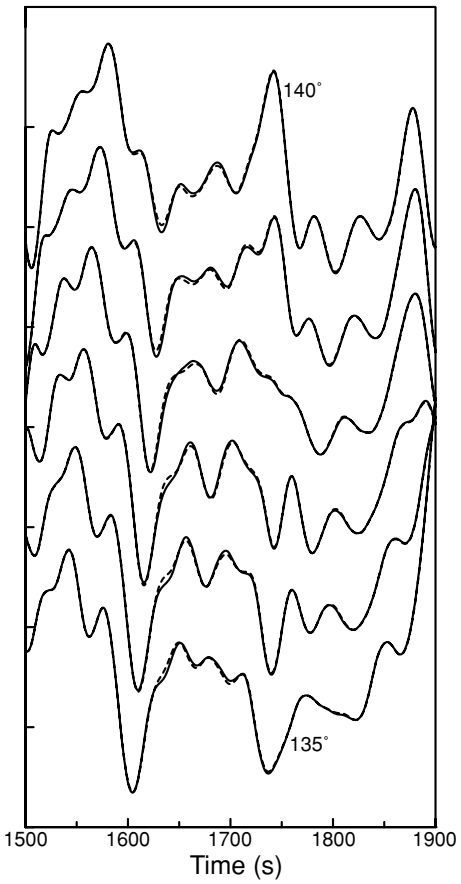

Figure 7. A comparison between synthetics computed for PREM (solid lines) with synthetics computed assuming an inner-core *S* velocity 10 per cent greater than PREM (dashed lines) at epicentral distances between 135 and 140°.

reduced at short periods because of mantle attenuation. It is this effect that causes the core phase *PKKP* to be much more visible in stacks of short-period seismograms compared to stacks of long-period seismograms (e.g. Astiz *et al.* 1996). Thus in future work it would be worthwhile to explore the relative visibility of *PKJKP* for plausible inner core models compared to the interfering mantle phases in both data and complete synthetic seismograms at a range of periods shorter than those examined here.

ACKNOWLEDGMENTS

We thank Arwen Deuss and an anonymous reviewer for their comments and suggestions. This work was supported by grant EAR-0710881 from the National Science Foundation. QL is supported by the Discovery grant of the Natural Sciences and Engineering Research Council of Canada and a University of Toronto Start-up fund. SEM simulations are done by the SPECFEM3D_GLOBE package downloadable from the Computational Infrastructure of Geodynamics (CIG) website http://www.geodynamics.org/cig/software.

REFERENCES

Astiz, L., Earle, P. & Shearer, P., 1996. Global stacking of broadband seismograms, *Seism. Res. Lett.,* **67,** 8–18.

Cao, A., Romanowicz, B. & Takeuchi, N., 2005. An observation of PKJKP: inferences on inner core shear properties, *Science,* **308,** 1453–1455, doi: 10.1126/science.1109134.

Chaljub, E., Capdeville, Y. & Vilotte, J.P., 2003. Solving elastodynamics in a fluid–solid heterogeneous sphere: a parallel spectral element approximation on non-conforming grids, *J. Comput. Phys.,* **187,** 457–491.

Cummins, P. & Johnson, L.R., 1988. Short-period body wave constraints on properties of the Earth's inner core boundary, *J. geophys. Res.,* **93,** 9058–9074.

Deuss, A., 2008. Normal mode constraints on shear and compressional wave velocity of Earth's inner core, *Earth planet. Sci. Lett.,* **268,** 364–375, doi: 10.1016/j.epsl.2008.01.029.

Deuss, A., Woodhouse, J.H., Paulssen, H. & Trampert, J., 2000. The observation of inner core shear waves, *Geophys. J. Int.,* **142,** 67–73.

Doornbos, D.J., 1974. The anelasticity of the inner core, *Geophys. J. R. astron. Soc.,* **38,** 397–415.

Dziewonski, A.M. & Anderson, D.L., 1981. Preliminary Reference Earth model, *Phys. Earth planet.Int.,* **25,** 297–356.

Dziewonski, A.M. & Gilbert, J.F., 1971. Solidity of the inner core of the Earth inferred from normal mode observations, *Nature,* **234,** 465–466.

Kawakatsu, H., 1992. Some attempt to observe PKJKP, *Central Core of the Earth,* **2,** 53–56.

Kawakatsu, H. & Niu, F., 1994. Seismic evidence for a 920-km discontinuity in the mantle, *Nature,* **371,** 301–305.

Komatitsch, D. & Tromp, J., 2002a. Spectral-element simulations of global seismic wave propagation – I. Validation, *Geophys. J. Int.,* **149,** 390–412.

Komatitsch, D. & Tromp, J., 2002b. Spectral-element simulations of global seismic wave propagation – II. 3-D models, oceans, rotation, and self-gravitation, *Geophys. J. Int.,* **150,** 303–318.

Koper, K.D. & Pyle, M.L., 2004. Observations of PKiKP/PcP amplitude ratios and implications for Earth structure at the boundaries of the liquid core, *J. geophys. Res.,* **109,** doi: 10.1029/2003JB002750.

Masters, T.G. & Shearer, P.M., 1990. Summary of seismological constraints on the structure of the Earth's core, *J. geophys. Res.,* **95,** 21 691–21 695.

Okal, E.A. & Cansi, Y., 1998. Detection of PKJKP at intermediate periods by progressive multi-channel correlation, *Earth planet. Sci. Lett.,* **164,** 23–30.

Shearer, P.M., 1990. Seismic imaging of upper-mantle structure with new evidence for a 520-km discontinuity, *Nature,* **344,** 121–126.

Shearer, P.M., 1991. Constraints on upper-mantle discontinuities from observations of long-period reflected and converted phases, *J. geophys. Res.,* **96,** 18 147–18 182.

Shearer, P. & Masters, G., 1990. The density and shear-velocity contrast at the inner core boundary, *Geophys. J. Int.,* **102,** 491–498.

Wookey, J. & Helffrich, G., 2008. Inner-core shear-wave anisotropy and texture from an observation of PKJKP waves, *Nature,* **454,** 873–876, doi: 10.1038/nature07131.